Simulation Refinements of European Reusable Staged-Combustion Rocket Engine SLME

Martin Sippel, Steffen Callsen, Ingrid Dietlein, Sina Leib
Martin.Sippel@dlr.de Tel. +49-421-244201145
Space Launcher Systems Analysis (SART), DLR, Bremen, Germany
Vasileios Pastrikakis, Valentyn Barannik, Theunis du Toit, Leonid Moroz
SoftInWay Switzerland GmbH, Baarerstrasse 2, Zug, Switzerland
Vasileios.Pastrikakis@softinwayswitzerland.ch Tel. +41-44-586-1998

The full-flow staged combustion cycle rocket engine with a moderate 15 to 17 MPa range in nominal chamber pressure called SpaceLiner Main Engine (SLME) has been under investigation by numerical simulations since several years. The SLME is today not only foreseen as the SpaceLiner's main propulsion but also used as reference for closed cycle LOX-LH2-engines in several studies of future European RLV. The launcher system high-level requirements on the main propulsion system as well as the engine system level requirements have been defined by DLR.

The Swiss company SoftInway and DLR successfully completed in 2024 a de-risk study under contract to the European Space Agency (ESA) to preliminarily consolidate a staged combustion engine design. Major findings of the pre-design of the turbomachinery, valves and lines, preburners and main combustion chamber, regenerative cooling using the commercial AxSTREAM® Platform and DLR-tools are summarized in the paper.

Contributions to the next iterative design step are addressed via refined simulations. The steady-state cycle analyses are improved on the powerhead side to mitigate certain shortcomings of the previous model. SoftInway's predesign data of the AxSTREAM® turbo-machinery sizing and heat-transfer analyses using engineering tools like TDK support the refinement of this updated engine cycle modelling. The study is complemented by simplified simulations of an engine control architecture for nominal sequences of operations.

Nomenclature

c*	characteristic velocity	m / s
I_{sp}	(mass) specific Impulse	s (N s / kg)
M	Mach-number	-
T	Thrust	N
m	mass	kg
ε	expansion ratio	-

Subscripts, Abbreviations

BL	Boundary Layer
FADEC	Full Authority Digital Engine Control
FFSC	Full-Flow Staged Combustion
FRSC	Fuel-Rich Staged Combustion
FTP	Fuel Turbo Pump
IHPRPT	Integrated High Payoff Rocket Propulsion Technology
LH2	Liquid Hydrogen
LOX	Liquid Oxygen
MCC	Main Combustion Chamber
MECO	Main Engine Cut Off
MR	mixture ratio
NPSP	Net Positive Suction Pressure
MSFC	Marshal Spaceflight Center (of NASA)
OTP	Oxidizer Turbo Pump
RLV	Reusable Launch Vehicle
SLB	SpaceLiner Booster stage
SLME	SpaceLiner Main Engine
SLO	SpaceLiner Orbiter stage
SLP	SpaceLiner Passenger stage
SSME	Space Shuttle Main Engine
TET	Turbine Entry Temperature
TRL	Technology Readiness Level
UDMH	Unsymmetrical Dimethyl Hydrazine
VTHL	Vertical Take-off and Horizontal Landing
VTVL	Vertical Take-off and Vertical Landing
C	chamber
s/l	sea level
vac	vacuum

1 INTRODUCTION

While the full-flow staged combustion cycle rocket engine SLME (SpaceLiner Main Engine) has been quite unique until recently in its FFSC-architecture, now a surprising number of proposals have come-up in Europe sharing similar thrust-levels and closed cycle flow schematics. Many of the proposals seem to be inspired by the SpaceX high-performance FFSC-engine Raptor (see DLR analyses in e.g. [1, 16]). One key difference remains: The SLME with its moderate 15 to 17 MPa range in chamber pressure (see investigations and numerical simulations in references [2 - 9]) is using hydrogen as fuel while the other European proposals select hydrocarbons, like e.g. methane.

The challenges of using low-density hydrogen are well known, as are its clear advantages in terms of superior performance and minimized atmospheric pollution when burned with LOX. The SLME originally defined as the baseline propulsion system for the reusable rocket-based high-speed intercontinental passenger transport concept SpaceLiner, is now also used as a reference for closed cycle LOX-LH2-engines in several studies of

future European RLV (see summary in [9] and a more detailed description of both VTVL and VTHL RLV-applications in e.g. [10 - 15]).

A partially similar staged combustion LOX/methane-engine in a range from 2000 kN up to 2500 kN is now under investigation in France under the name PROMETHEUS-X [19]. A similar high-performance 2200 kN LOX-LH2-engine is under development in China for propulsion of China's heavy launch vehicle core [20]. The ESA "THRUST!"-initiative is funding extensive exploratory activities on closed cycle engines led by The Exploration Company (TEC) and Pangea.

2 SLME DEFINITION STATUS

Staged combustion cycle rocket engines around a moderate 16 MPa chamber pressure were chosen early in the SpaceLiner definition [2, 9]. This level is not overly ambitious and has already been exceeded by operational values of engines like SSME or RD-0120 [9]. The target of 16 MPa is also a good compromise between European expertise [21] and required performance of future launcher applications. The intended demonstrator SCORE-D [22] was the latest ESA-funded design and experimental work on maturing closed cycle LOX-LH2-rocket engines. The design chamber pressure would have been 15 MPa [9].

The expansion ratios of the SpaceLiner booster and upper stage engines are to be adapted to their respective optimums; while the mass flow, turbo-machinery, and combustion chamber are intended to remain identical as far as possible and useful. This approach would allow for significant reduction in development-, testing-, and production costs. In certain applications with an expendable upper stage (see e.g. [9, 11, 12, 13, 14, 17]) the reusable booster engines might perform a final mission with additional nozzle extension when approaching its design life-time.

This section summarizes the historical background, lists the newly defined high-level and engine system requirements, followed by describing cycle conditions and latest preliminary sizing of components for the SLME with nozzle expansion ratios 33. The upper stage variant with ε=59 mainly differ in slightly changed nozzle area ratios but will function with very similar internal operating conditions. Therefore, the preliminary component designs are relevant independent of nozzle expansion ratio.

2.1 Previous SLME analyses and historical perspective

Historically, very few staged combustion engines of the Full-Flow sub-cycle have been realized. Only two non-European FFSC engines have ever been developed which are based on different propellant combinations: The RD-270 (8D420) was the first ever full flow staged combustion rocket engine and was designed and produced by Energomash between 1962 and 1970 [23]. The propellants used were UDMH and N_2O_4 and the targeted chamber pressure was 26.1 MPa. The RD-270 was tested between 1967 and 1969 but never flown. The other engine is the SpaceX Raptor (2) [1, 16] based on LOX-LCH4 propellants which is currently in its flight testing with the intended fully reusable Starship&-SuperHeavy launcher.

However, in the US the Integrated High Payoff Rocket Propulsion Technology (IHPRPT) research program has spent significant resources on the FFSC-cycle and in particular for LOX-LH2 propellants. The program was instituted as fifteen-year rocket propulsion technology improvement initiative by US Air Force, Army, Navy, and NASA [26]. Eventually, in 2013 an Integrated Powerhead Demonstration reached 100% power level at NASA's Stennis Space Center [28].

Already before, an FFSC derivative engine of the SSME had been proposed [24] to be operated as a highly variable mixture ratio engine, especially for booster applications. A very compact lay-out of the IPH-Ox with annular preburner around the shaft connecting turbine and impeller was intended. References 7 and 24 show the design of the projected SSME "Derivative Engine" ox-rich power head.

Such advanced designs are probably essential for the success of FFSC-types. Reference 27 performs a systematic assessment of all sub-cycle variants of LOX-LH2 staged combustion engines and lists the major thermodynamic advantage of FFSC as "*allowing a significant increase in the powerhead energy release within the same turbine temperature limits. […] The overall effect is approximately a 10% to 15% improvement in chamber pressure of the full-flow cycle over the conventional [FR] cycle combined with lower turbine temperatures.*". However, at the downside [27] mentions "*full-flow dual preburner cycle options have reduced sea level thrust-to-weight due to the significant weight of the oxidizer rich preburner and 02-rich hot gas manifold*".

The latter can be drastically reduced or even completely eliminated if the ox-rich power head is designed as presented in [24, 25] and potentially mounted directly on top of the main combustion chamber as realized with Raptor.

The most suitable mixture ratio range of the SpaceLiner main propulsion system along its passenger mission has been defined by system analyses optimizing the full trajectory. Nominal engine MR control at two engine operation points (6.5 from lift-off until reaching 2.5 g acceleration and 5.5 afterwards) has been found most promising [2].

Two types of staged combustion cycles (one full-flow and the other fuel-rich) have been considered for the SLME and traded by numerical cycle analyses [2, 3]. A Full-Flow Staged Combustion Cycle with a fuel-rich preburner gas turbine driving the LH2-pump and an oxidizer-rich preburner gas turbine driving the LOX-pump remains the preferred design solution for the SpaceLiner [6].

2.2 SLME design requirements

The de-risk study partially funded by ESA has been initiated with consolidation and numbering of SLME key design requirements on mission level or High-Level Requirements (HLR) and derived Engine System Requirements (ESR). The performed preliminary sizing has been based on specific numbers. In case these values could change in future variations or trade-offs, the numbers are still preliminary and set in brackets [ ].

2.2.1 High-Level Requirements (HLR)

The SpaceLiner 7 take-off thrust requirement per engine of around 2000 kN at sea-level conditions remains unchanged to [6, 7]. The nominal operational mixture ratio range reaches from 6.5 to 5.5 with MR of 6.5 in the early flight phase and subsequent throttling to 5.5. Other investigated RLV-applications pick simply one of these operating points and keep MR constant along the full mission. Deep-throttling down to 35% of sea-level thrust (≈740 kN) would be mandatory only for the vertical landing of VTVL-concepts. This demanding value has explicitly *not* been included in the HLR-list and should only be added if needed by selected vehicles.

Table 1: High Level Requirements

	Description
HLR 1	Propellant combination should be LOX-LH2 in suitable MR-range.
HLR 2	Thrust level should be 2200 kN in vacuum condition.
HLR 3	Thrust level should be throttleable at least in range 93% - 107%
HLR 4	Engine should be capable of [25] flight-mission reuses.
HLR 5	Design of engine components should consider state-of-the-art low-cost manufacturing technologies.
HLR 6	Engine should use FADEC and electric actuators when possible and collect operating data in HMS.
HLR 7	Reliability of engine should reach [1-1.e-4] and availability should reach [1-1.e-4]
HLR 8	Engine should reach Initial Operational Capability (IOC) in [2035]

The average engine life-time is targeting 25 missions (HLR 4) or cycles with limited refurbishment effort. The SLB engine thus requires an accumulated operational time of 6100 s (1.7 h). The upper stage engine for SLP and SLO is aiming for almost 11600 s (3.2 h) with 2h 20 minutes at a demanding MR of 6.5. These values demonstrate the technical challenges of realizing a safe and cost-efficient reusable rocket engine.

The next generation of partially reusable launchers will see similar operation times and conditions on the RLV-stages but significantly less-demanding environments on the expendable upper stages. In case of VTVL an in-flight reignition capability of up to 4 times per mission would be required while for all other applications a single ignition per mission is sufficient. Multiple ignitions per missions are not an HLR, similar to deep-throttling. Instead, a double ignition capability of the main combustion chamber and preburners is defined as an optional engine system requirement (ESR 12).

2.2.2 Engine System Requirements (ESR)

The first system requirement is the closed-cycle engine and the second (ESR2) already defines the FFSC as the preferred choice. This approach should allow avoiding the complexity and cost of additional inert gases like Helium for sealing. The additional power of the ox-rich flow enables lower turbine temperatures and hence less stress, translating into longer turbine life, a key factor for reusable rocket engine life [25, 27].

Typical accumulated life time requirements of the SLME are defined in ESR10, derived of the SpaceLiner's ascent reference mission mentioned in [8]:

- Nominal operation time of Booster engine: 245 s with 122 s @ MR=6.5 and 122 s @ MR=5.5 or earlier cut-off
- Nominal operation time of Passenger Stage engine: 463 s with 336 s @ MR=6.5 and 127 s @ MR=5.5

Table 2: Engine System Requirements

	Requirement description
ESR 1	Engine should be a high-performance closed-cycle.
ESR 2	Preferred sub-cycle solution should be Full-Flow Staged Combustion (FFSC) with 2 pre-burners, one oxidizer-rich, one fuel-rich serving main combustion chamber (MCC) only with fluids in gaseous state
ESR 3	Preliminary cycle scheme: see Figure 1
ESR 4	Main combustion chamber pressure in reference operating point should be 16 MPa
ESR 5	Nozzle supersonic area ratio of reference engine for 1st- / booster-stage operations should be around 33
ESR 6	Engine (following ESR4 & ESR5) weight should target T_{vac} / W of 75
ESR 7	Engine should stay compact and it should be avoided that any subsystem, harness, line or turbomachinery component is extending outside an envelope cylinder extruded upward from the nozzle exit plane
ESR 8	Engine should be capable of being adapted to derived version[s] applied to upper-stage operation using nozzle with increased area ratio without major design changes upstream of [nozzle throat]
ESR 9	Engine mixture ratio (MR) should be variable for nominal operating points in the range 5.5 – 6.5 and off-nominal range should extend to at least 5 – 7
ESR 10	Typical engine operation time per mission should be up to 250 s (1st stages application) and up to [500] s (upper stage application) – accumulated life time 6250 s or [12500] s
ESR 11	Expendable variant of upper stage engine could be an option, potentially built out of modified used 1st stage engines reaching accumulated life time [3000] s
ESR 12	Engine should have multiple ignition capability on pre-burners and MCC up [2] times per flight
ESR 13	Maintenance and refurbishment effort of engine between flights should be minimized and not exceed [5 tbc] % of production costs.
ESR 14	Engine propellant-supply interface conditions should be for H2 [0.2 MPa, 20.5 K] and for O2 [0.5 MPa, 90.5 K]
ESR 15	Engine operation should be stable in the defined operational domain and any nominal operation point should be continuously reached within [5 s]
ESR 16	Engine should be capable of providing GH2 at [1.1 kg/s, 10 MPa, 180 K] and GO2 at [1.5 kg/s, 10 MPa, 150 K] for propellant tank pressurization
ESR 17	He-consumption of engine should be minimized and major portion of He should be recovered on ground during purge-procedures prior to chill-down [> 85% tbc].
ESR 18	Startup transient of engine to 100% stable thrust level should take [< 3.5 s]
ESR 19	Shut-down transient of engine from 100% thrust level to [< 10%] thrust level should take [< 5 s]
ESR 20	Engine controls should be fully autonomous and redundantly accept high-level flight control commands

ESR 21	Engine thrust vector should be capable of being controlled by TVC around y- and z-axis within specifications [TBC +/- 8° , tbc 15°/s, TBD °/s2]

The minimum NPSP has been set to 70 kPa for the LH2-boost pump, and to 230 kPa for LOX-inducer pump based on comparable engine designs.

2.3 SLME Functional Architecture

A Full-Flow Staged Combustion Cycle (FFSC) with a fuel-rich preburner gas turbine driving the LH2-pump and an oxidizer-rich preburner gas turbine driving the LOX-pump is the preferred design solution for the SLME (ESR 2). The components and their connections are shown in Figure 1 for the current baseline with FTP split into boost pump driven by separate expander turbine and HPFTP. The HPOTP is a combination of inducer- and impeller-stage driven by the same oxidizer-rich turbine.

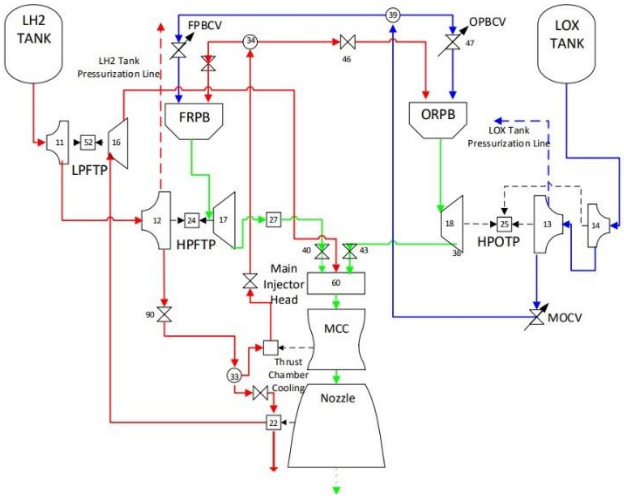

Figure 1: SLME internal flow schematics

In a Full-Flow Staged Combustion Cycle, two pre-burners whose mixture ratios are strongly different from each other generate turbine gas for the two turbo pumps. All of the fuel and oxidizer, except for the flow rates of the tank pressurisation, is fed to the fuel-rich preburner (FRPB) and the oxidizer-rich preburner (ORPB) after being pressurised by each turbo pump. After the turbine gases created in each preburner drive the respective turbine they are all injected in hot gaseous condition into the main combustion chamber (MCC). The regenerative cooling of the chamber and the nozzle is performed with the hydrogen fuel after being discharged by the HPFTP [2, 3].

2.4 Preliminary subcomponent sizing

Subcomponent sizing and definition is progressing at Phase A conceptual design level with major progress achieved in the ESA de-risk study. The key-objective is a light-weight, long-life, low-maintenance architecture. This section gives a summary of the milestone definition reached at the end of 2024.

2.4.1 Thrustchamber and regenerative cooling circuit

The geometry of the thrustchamber including chamber and nozzle had been calculated by the DLR tool ncc on the basis of the designed combustion condition (mixture ratio, combustion pressure, fuel flow rate, combustion efficiency) and geometry parameters (contraction ratio, expansion ratio, characteristic chamber length, entry and exit angles of the contour). The booster engine and the orbiter engine have the same geometry in the chamber part including the throat, but not the same in the supersonic expansion part of the nozzle. The nozzle for the orbiter engine does not only have a larger expansion ratio but also a smaller nozzle entry angle. This allows for reduced flow divergence by a smaller exit angle.

The thrustchambers' internal flow contours as presented in [5, 6] have remained the baseline for the SLME up to the de-risk study. Only very recently the flow contours are critically reassessed in the refined simulations briefly described in the following section 2.5.3.

The thrustchamber cooling baseline has been described in [7, 8]: H_2 regenerative and film cooling are combined for the booster engine. Supercritical H_2 of the HPFTP discharge adapted to around 30 MPa is split into two separate passes both induced in the supersonic section at expansion 4.5 (Figure 2). One counter flow pass in segment S1 (approximately 2/3 of total flow) chills the chamber including the throat area and the other pass in S2 chills the nozzle area downstream up to expansion of 16.6. Most of this flow is directed to power the LPFTP expander turbine. Further downstream in segment S3 a combination of small bleed and radiation is used for cooling. Fuel for film cooling is supplied from the LPFTP at the injector plate's outward ring, further chilling the chamber wall.

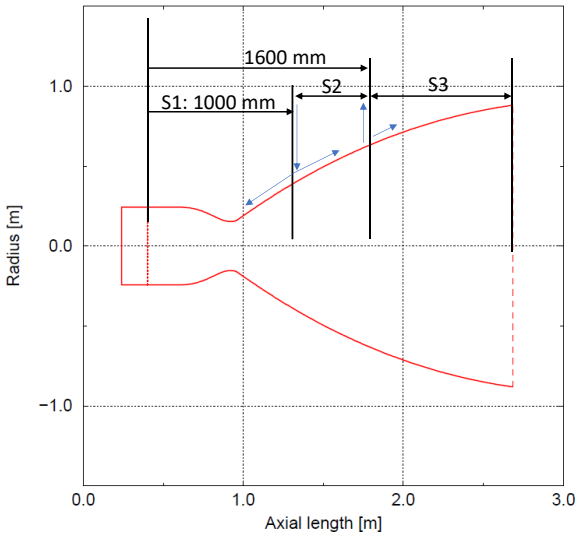

Figure 2: Regenerative cooling concept of SLME with nozzle expansion 33

A thin thermal barrier coating is applied to the wall facing the hotgas to avoid excessive temperatures of the chamber wall material. Thus, thermal stresses and low cycle fatigue effects are reduced, improving the thrust-chamber lifetime.

A preliminary thermal analysis of the SLME on the hot-gas side had been performed [7, 8] using the program RPA [31] offering a thermal analysis module for different types of thrustchamber cooling methods, including radiation, convective (regenerative) and film cooling. The accuracy is claimed to be sufficient for conceptual and preliminary design studies, as well as for rapid evaluation of different channel variants. [31, 32] The hot

gas properties for thermal analysis are retrieved from a quasi-one-dimensional flow model.

SoftInWay had performed a new, independent cooling analysis of the main combustion chamber and nozzle in the ESA-supported de-risk study for the nominal operating point O1. The properties of the working fluids and structural materials are taken from the AxSTREAM® material library that contain different real fluids databases like NIST *Refprop* [35] or *Coolprop* [34] Zirconium Copper was selected as the internal wall material, since it does not become embrittled at low temperatures and has a high thermal conductivity coefficient. The one-dimensional analysis was performed using the AxSTREAM® system simulation software. The thrustchamber has been discretized into 18 sections (11 in S1, 3 in S2, 4 in S3) with geometrical parameters kept constant in each section.

Figure 3 shows wall temperatures along the thrustchamber considering regenerative cooling as well as film cooling. The maximum wall temperatures found remain at less than 800 K in this simulation. This corresponds to a peak heatflux of 110 MW/m^2 at the throat. Figure 4 depicts the H_2 coolant temperature evolution in the channels consistent with the above assumptions.

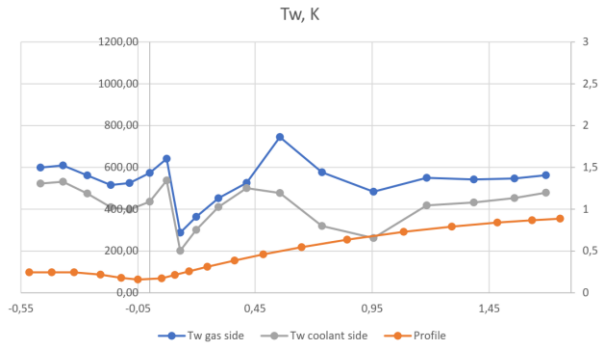

Figure 3: Wall temperature distribution in SLME-33 thrustchamber at O1 obtained from AxSTREAM® analysis

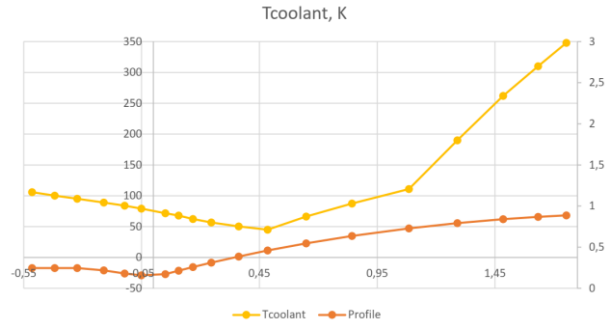

Figure 4: Coolant total temperature in SLME-33 thrustchamber at O1 obtained from AxSTREAM® analysis

An exploration of different operating points had been previously performed with RPA in order to check on the feasibility of the regenerative cooling concept in the full operational domain, see [7, 8]. In the upper stage version of the SLME with expansion ratio 59 the chamber cooling strategy is currently assumed very similar to the version with smaller nozzle extension [8].

For the main combustion chamber a coaxial injector type is selected similar to other oxygen-hydrogen engines. In the de-risk study SoftInWay refined the previous design (see [5, 6]) to relatively high flow-rate elements. The faceplate is equipped with 169 coaxial injector elements fed from the preburners with massflow rates of up to 3.25 kg/s and flow ratio (ox-rich to fuel-rich gas) between 2.5 and 3.75. Note, the injector is operating in gas-gas mode which is simplifying the mixing and enhancing combustion stability. The high flowrate injectors are surrounded by 89 smaller injectors adjacent to the wall fed with supercritical hydrogen from the LPFTP turbine for film cooling. The preliminary assembly of the injector and the dome is visible in Figure 5.

A spark igniter placed in the center of the injector head is reference for the SLME, similar to the SSME design [36]. Note, the igniter is not shown in the layout in Figure 5.

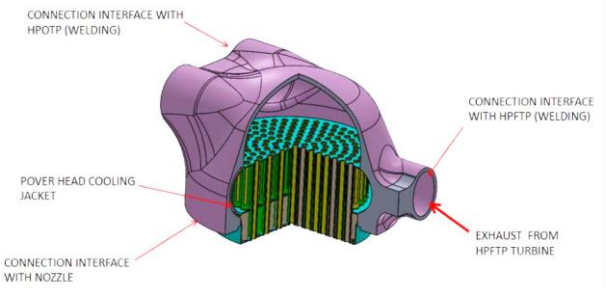

Figure 5: CAD-assembly of injector head and dome as designed by SoftInWay

2.4.2 Integrated Power Head

An Integrated Power Head (Pre-burner + Turbine + Impeller pump) as it has been used on the SSME (see figure in [9, 36]) was the baseline design for the SLME. However note, the cycle architectures of SSME and SLME differ with the former using two fuel-rich preburners to power the turbines. The de-risk study revealed that FFSC makes a difference to the preferred IPH-architecture and a different arrangement might be preferrable (see section 2.7). Still, the description in this section is summarizing the consolidated design of merely the baseline.

Figure 6 shows for the 2024 reference variant now called V7 the integration of all major components of the Integrated Power Head in the upper section of the SLME and their integration with the combustion chamber injector head following the SSME example. The preliminary layout already described in [8] was maintained integrating the refined turbopumps sizing (section 2.4.4) and a preliminary definition of mechanical architecture including iterative adaptation of the hot and cold fluid lines (section 2.4.5).

The view of the SLME-33 from above in Figure 6 shows on the right the hydrogen fuel supply and on the left the oxygen flow interface.

The OR-IPH-assembly is a classical turbopump architecture with the pump impeller and turbine seated on a single shaft housed in the turbopump casings with the preburner placed at the top end of the assembly prior to the turbine stator and rotor. The FR-IPH consists in a similar way with the FRPB positioned on top of the HPFTP (Figure 7).

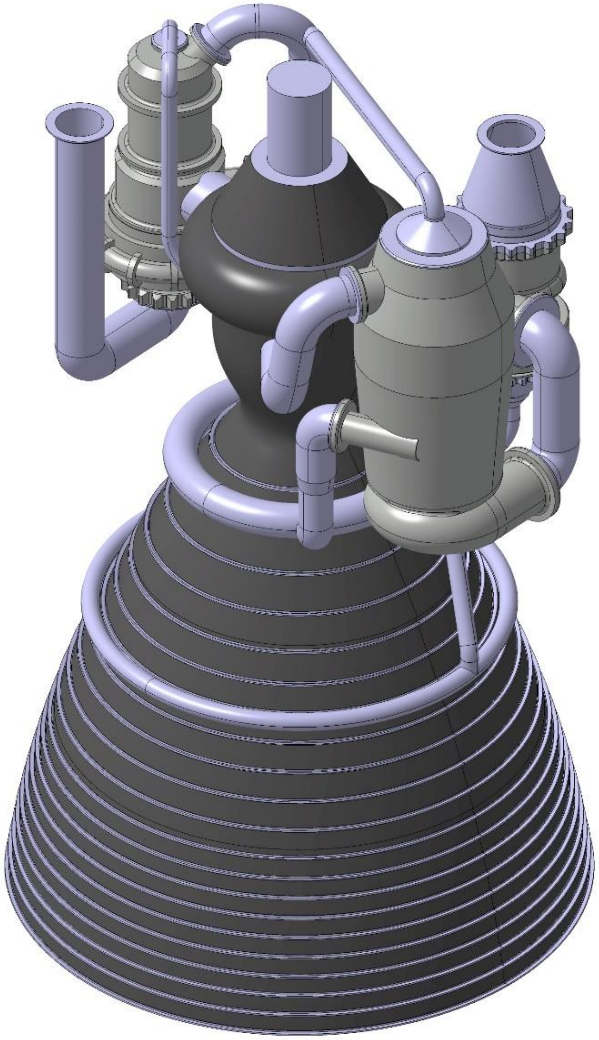

Figure 6: SLME V7 simplified CAD geometry with arrangement of turbomachinery

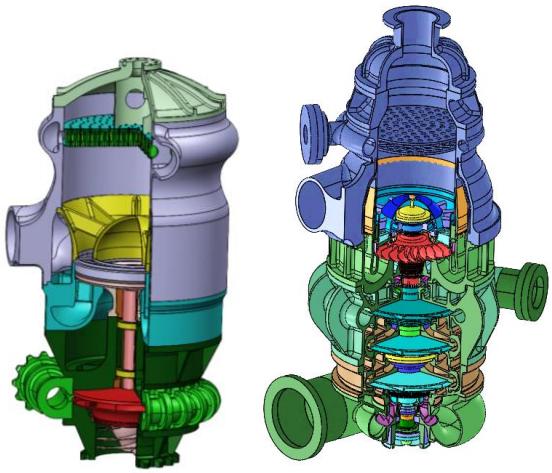

Figure 7: SLME simplified CAD geometries of oxygen-rich-IPH (left) and fuel-rich-IPH (right) in SiW design proposal

Note, the OR-IPH as shown in Figure 6 is of different lay-out than the one presented in Figure 7 left.

2.4.3 Preburners

The mixture ratios of the fuel-rich preburner (FR-PB) and the oxidizer-rich preburner (OR-PB) are controlled to be less than 1.0 and above 120 so that TET is restricted to acceptable values (see section 2.5.2). The full-flow sub-cycle allows TET remaining in a small range from 730 K to 770 K, even in the extreme domain, without excessively raising preburner pressures. The limitation of the nominal characteristic conditions should enable an engine lifetime of up to 25 flights. Further, this approach gives some margin to significantly raise engine power in case of extreme emergencies by increasing TET beyond the defined limits [2]. However, mission and systems-analyses of the SpaceLiner configuration show that such extreme measures might not even be required due to good robustness and performance margins of the vehicle [18].

The standard sizing methodology as used by SiW resulted in a relatively large OR-preburner with diameter close to that of the main combustion chamber. This concept out of Inconel becomes heavy. Some trades on alternative designs have been performed in the de-risk activities and an engineering sizing was performed by applying suitable propellant residence times according to [37]. Ignition of LOX with H_2 at high mixture ratios is hardly possible (see e.g. [26]). Therefore, a different approach with central hot primary zone at standard MR and cold, circumferential wall zone with O_2-flow is proposed. These initially coaxial flows need to be mixed that the temperature field at turbine entry plane is adequately homogeneous. A turbulent mixing zone with forced turbulence for mixing the hot H_2O with O_2 is required. A design with similarities to cross- or reverse-flow gas generators seems to be promising [26, 37]. However, further research will be necessary to reach mature design stage of the concept.

2.4.4 Turbomachinery

The first preliminary definition of the turbomachinery lay-out has been described in references 3 through 7. On the fuel side a boost pump driven by an expander turbine fed from the regenerative circuit is feeding the HPFTP. On the LOX-side a conventional HPOTP with inducer and single stage impeller on the same shaft is proposed powered by a single stage turbine. In case of the preferred full-flow staged combustion cycle the LOX-split pump is eliminated because unnecessary for raising discharge pressure to the fuel-rich preburner level as with the SSME [36].

A refinement of the SLME turbomachinery design was performed within the de-risk study for ESA using the AxSTREAM® platform developed by SoftInWay (SiW).

AxSTREAM® is a multidisciplinary design, analysis and optimization software platform that provides fully integrated and streamlined solutions, encompassing the complete turbomachinery design process, all in a seamless interactive user interface. Preliminary estimation of performance and dimension of turbomachinery components are done with the generative design module that is based on an inverse task solver and allows generation of thousands of geometry options within seconds for users to review data and compare at design- and off-design conditions.

According to the cycle flow scheme shown in Figure 1, the following turbomachinery components have been pre-designed: LPFTP pump and turbine, HPFTP pump and turbine and HPOTP pump and turbine. The thermo-

dynamic parameters used for the turbomachines design correspond to the operational point O1 and the SLME cycle design conditions of 2022 as presented in [8].

AxSTREAM® turbomachine internal efficiency accounts for flow path quality, tip and back face leakage losses and disk friction losses without considering mechanical losses.

LPFTP

The boost pump is used to pressurize the hydrogen fuel before its entry into the HPFTP. Increasing the cavitation margins of the fuel-fed system allows decreasing of tank pressure. Fuel from the tank enters the boost pump flow path with a minimum pressure of 0.176 MPa and is pressurized to 1.5 MPa at O1.

An inducer (diagonal) type of wheel is used as the preferred pump concept. The rotational speed and several main geometrical parameters have been varied to generate the design space of feasible configurations that satisfy the required cavitation margin. Figure 8 shows the design in a 3D-view.

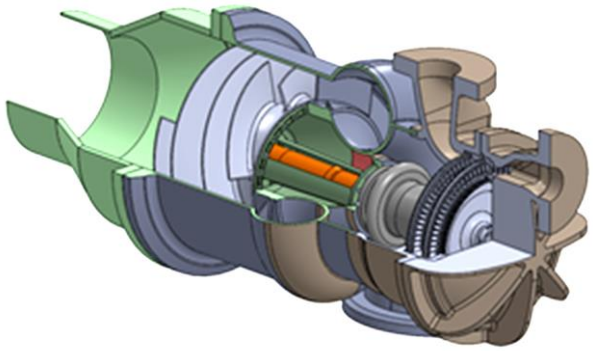

Figure 8: SLME LPFTP in SiW preliminary design

Performance parameters of the LPFTP are presented in Table 3.

Table 3: SLME LPFTP pump preliminary design characteristics in nominal range O1, O2, O3

Operational Point	O1	O2	O3
Mass flow rate [kg/s]	75.7	76.3	75.9
Power [kW]	1766	1981	1769
Pressure ratio [-]	8.5	9.4	8.5
Axial length [mm]	351		
Maximal diameter [mm]	444		

The turbine is fed from the regenerative circuit segment S2 (see Figure 2) with hydrogen gas to drive the boost pump. The expander-type turbine driven by heated hydrogen is designed to cover pump power requirements considering mechanical losses. As it is supposed to use a single shaft turbopump, the shaft rotational speed corresponds to the one determined for the pump.

A few turbine design options were considered by SiW. The maximum efficiency considering the geometrical restriction of maximal LPFTP casing diameter preliminarily set to generous 444 mm was achieved for double stage impulse design with partial admission ratio about 0.12.

Main performance and dimensions data of the LPFTP turbine are given in Table 4.

Table 4: SLME LPFTP turbine preliminary design characteristics in nominal range O1, O2, O3

Operational Point	O1	O2	O3
Mass flow rate [kg/s]	9.9	10.6	9.8
Power [kW]	1812	2035	1815
Axial length [mm]	55		
Maximal diameter [mm]	224		

Preliminary selection of materials for the LPFTP are Al 7075, 15-5PH(S15500) and AlLi A356.0 which have been used for the structural pre-sizing. Reference [9] presented some FEM-results of studied rotor and blade design options of the LPFTP turbine and pump.

Size and weight of the preliminary SLME LPFTP assembly is relatively large compared to the SSME (see [36]). A more compact and lighter design might be preferable in future SLME maturation at the expense of somehow reduced efficiencies.

The full scope of rotor dynamic analyses according to API standards [40] was performed for all turbopumps. The critical speed map for LPFTP and the LPFTP mode shape corresponding to the first bending critical speed has been presented in [9].

HPFTP

The pressurized flow after the LPFTP enters the HPFTP pump. The HPFTP outlet pressures are depending on the operation point, between 32.2 MPa and 35.8 MPa. Several design configurations of the HPFTP pump were initially considered varying the inducer, the vane diffuser presence, and the number of stages. The configuration and parameters are to be selected specifically under consideration of their impact on the cavitation margin, the efficiency, and the dimensions of the designed pumps. Additionally, a casing diameter constraint had been proposed at 500 mm which had to be relaxed to 560 mm.

A 3-stage impeller HPFTP pump is considered as the baseline configuration, while satisfying the casing diameter constraint. Figure 9 represents the 3D-drawing of the HPFTP.

All centrifugal wheels contain the same blade profile. This choice helps significantly dropping the manufacturing cost without big impact on the flow path efficiency. Performance data of the HPFTP pump are presented in Table 5.

Table 5: SLME HPFTP pump preliminary design characteristics in nominal range O1, O2, O3

Operational Point	O1	O2	O3
Mass flow rate [kg/s]	75.7	76.2	75.9
Power [kW]	38710	41030	37994
Pressure ratio [-]	24.7	23.5	24.2
Axial length [mm]	425		
Maximal diameter [mm]	560		

The HPFTP turbine is driven by combustion gas from the fuel-rich preburner. Reaction turbine design is selected as the baseline as it provides the highest efficiency for the given isentropic velocity ratio. Maximum diameter restriction, stress limitations and relatively big blade height ($D_m/l \approx 5$) led to a stage design with suboptimal nozzle outlet angles that decreases the flow path efficiency. For flow paths with $D_m/l < 10$ a significant change of the flow parameters

(angles) along the blade span is observed, thus, a 3D blade design is preferable.

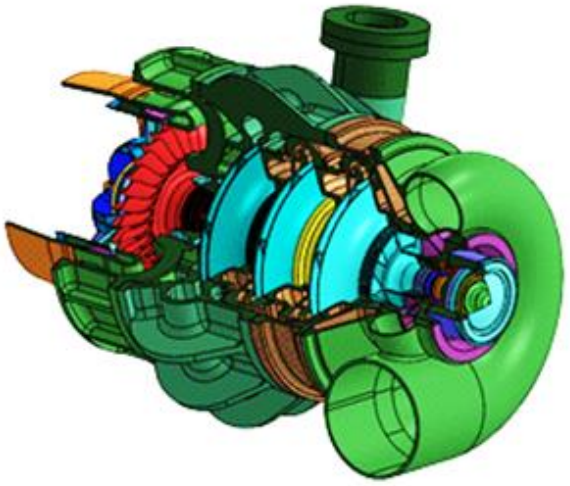

Figure 9: SLME HPFTP in SiW preliminary design

Table 6 represents the performance data of the HPFTP turbine.

Table 6: SLME HPFTP turbine preliminary design characteristics in nominal range O1, O2, O3

Operational Point	O1	O2	O3
Mass flow rate [kg/s]	98.1	101.2	95.9
Power [kW]	38710	41030	37994
Axial length [mm]	71.2		
Maximal diameter [mm]	275		

The selected materials for the HPFTP are Al 7075, Waspaloy, Inconel718, 15-5PH (S15500).

The full scope of rotor dynamic analyses according to API standards [40] was performed for all turbopumps. The critical speed map for LPFTP and the LPFTP mode shape corresponding to the first bending critical speed has been presented in [9]. The calculated separation margins to critical speeds are below the required values and a redesign of the HPFT is recommended for the future.

HPOTP

Oxygen is fed from the tank directly to the HPOTP with minimum interface pressure of 0.75 MPa and is to be pressurized between 28.2 MPa and 32.16 MPa according to cycle modeling. Thus, an inducer wheel is required to avoid any cavitation at the impeller stages. Two possible configurations were considered: single and double stage impeller on the same shaft with the inducer [8]. Maximal casing diameter of the HPOTP was initially tried not to exceed 350 mm.

The design with single stage impeller has been selected [8]. Preliminary design of both pumps shows that exceeding the external diameter target can't be avoided. The pump exit volute diameter is calculated at 538 mm and maximum external dimensions are 569 mm. The preliminary design of the HPOTP is presented in Figure 10.

Table 7 represents performance data of the HPOTP-pump.

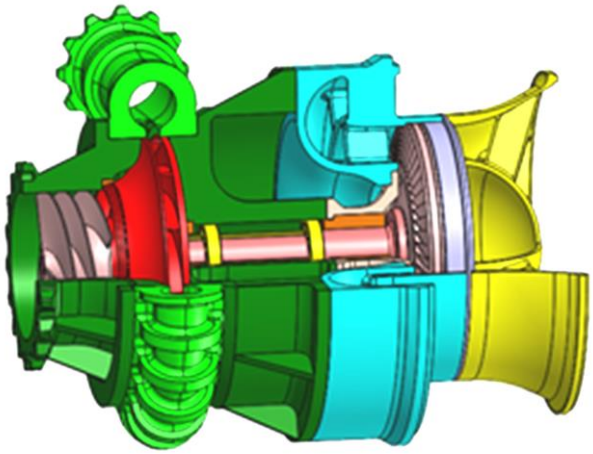

Figure 10: SLME HPOTP in SiW preliminary design

Table 7: SLME HPOTP pump preliminary design characteristics in nominal range O1, O2, O3

Operational Point	O1	O2	O3
Mass flow rate [kg/s]	445	486	409
Power [kW]	15127	17746	12906
Pressure ratio [-]	60.6	71.1	52.7
Axial length [mm]	197.4		
Maximal diameter [mm]	569		

The materials selected for the HPOTP pre-design are Al 7075, Waspaloy, Inconel718 and 15-5PH (S15500).

The HPOTP turbine is driven by the oxidizer rich gases from the oxidizer preburner. The preliminary design of the HPOTP turbine is adequate to meet the pump power requirement. A reaction design of the turbine with 3D blades is assumed to be optimal for the given boundary conditions.

Performance data of the HPOTP turbine is presented in Table 8. The critical speed map for the HPOTP has been presented in [9].

Table 8: SLME HPOTP turbine preliminary design characteristics in nominal range O1, O2, O3

Operational Point	O1	O2	O3
Mass flow rate [kg/s]	406	443	372
Power [kW]	15154	17775	12974
Axial length [mm]	65.1		
Maximal diameter [mm]	362		

2.4.5 Mechanical Architecture and Fluid Lines

The mechanical architecture of the SLME with arrangement of the complete turbomachinery, the connecting lines and bellows and the components attachment to the thrustchamber has been defined [9]. A classic rocket engine architecture is selected, although, alternatives with clustered turbomachinery serving different thrustchambers without being structurally attached to them [25] might be considered in the future for the multiple-engine launcher stages.

As first step, the fluid lines have been iteratively sized for required cross-sections to keep pressure losses at acceptable levels.

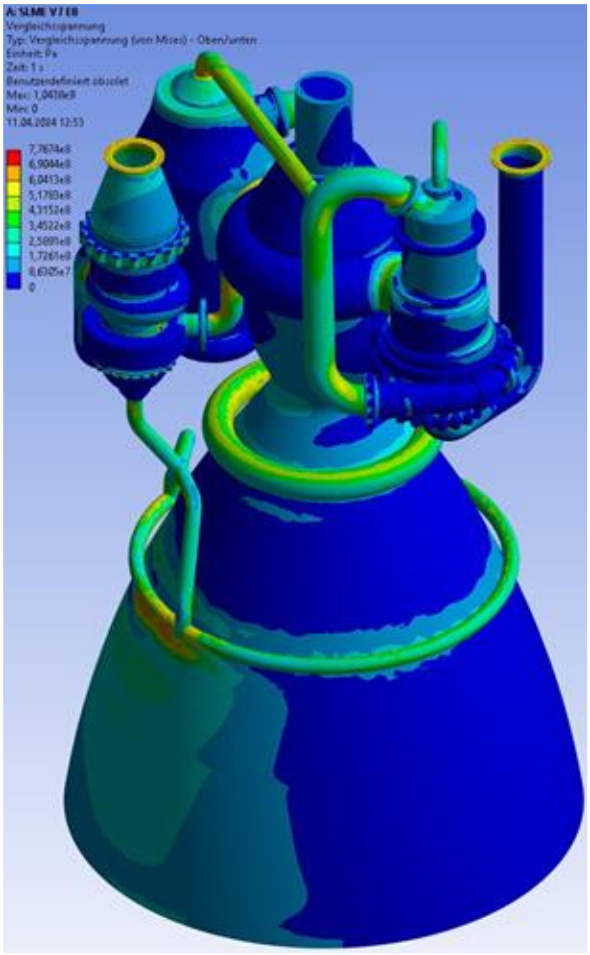

Figure 11: Von Mises stresses in SLME-33 lines at extreme operating point E8

Based on the dimensions and total conditions from cycle analyses, the static loads acting on the structure are calculated in the full domain for nominal and extreme operating points (see section 2.5). The material choice of all lines in the preliminary sizing has been Inconel 625 with consideration of temperature dependent properties. Stresses have been calculated using FEM with the commercial tool Ansys 2023 R1 for dimensioning load cases. An example of the obtained stresses after adjusting the wall thicknesses is shown in Figure 11. Note, only stress levels of lines are meaningful because thrustchamber and turbopump casings are strongly simplified and were not subjected to all relevant loads in the analyses.

Insulation has been applied to the H2-lines up to the supply torus of the regenerative circuit while the oxygen side does not require line insulation. Figure 12 shows the calculated wall temperatures under the theoretical assumption of power packs operating but without any heatloads from the main combustion chamber.

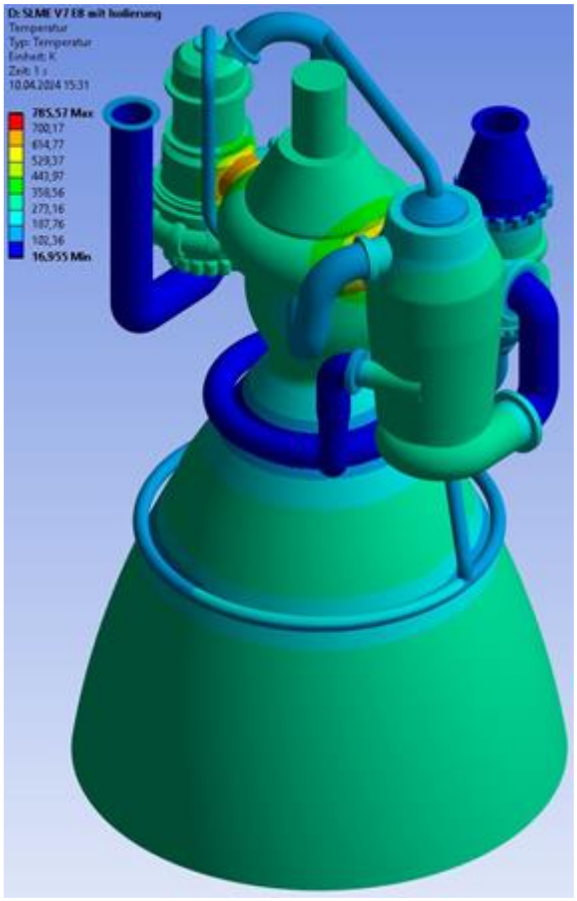

Figure 12: Wall temperatures in SLME-33 lines from thermal analysis

2.4.6 Engine Controls and HM

The SLME engine controls and actuation system is intended to be designed fully electric for maximum safety and manufacturing cost reduction. A FADEC system as in modern aircraft engines centralizes all HM-information and has a redundant data link to the vehicle's flight control and data management and data handling.

Preliminary work is currently performed with the purpose to define an actuator and control logic for the steady-state regime of the SLME. A first cast of a potential control scheme is shown in Figure 13. It is similar to [41] but yet simplified at this stage of work. The engine monitor unit would collect and interpret sensor information and evaluate them. The purpose is to identify component and system level parameters, verify that the observed parameter range is within reasonable limits in terms of durability and safety, and generate data from sensor measurements used for motor control. As such it encompasses the HMS but also acts towards the feedback loop of the control loop.

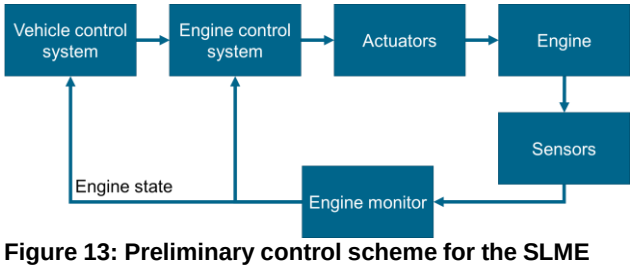

Figure 13: Preliminary control scheme for the SLME

Output from the engine monitor unit will be fed to the launch vehicle or SpaceLiner flight control system and to the engine controller. The former will formulate commands to the engine control system according to mission and vehicle needs and in accordance with high level requirements or when safety measures are to be taken e.g. reacting to engine-out events.

The proper operation of the engine and its components will be controlled by the engine control system for which the baseline concept, similarly to the Space Shuttle Main Engine (SSME) [36], has thrust control by the oxidizer-rich preburner control valve (OPBCV) whereas mixture ratio is controlled by the fuel-rich preburner control valve (FPBCV). Both only act upon oxidizer mass flow rate into the respective preburners as shown in Figure 1. The need for an additional main oxidizer control valve (MOCV) which is in series to the other two valves is under debate and will depend on the actual valve architecture and its operating range. The SSME has a valve and bypass to regulate the regenerative cooling flow. If such devices would be needed in the SLME requires more in-depth studies of the cooling flow characteristics and its dynamics.

Engine status data are provided by a suitable selection of sensor types. As preliminary assumption, combustion chamber pressure shall be monitored as much as temperatures and pressures at the low-pressure fuel pump outlet. These data shall be complemented by a volume flow meter at the low-pressure fuel pump discharge and temperature gauges at the turbine discharges for both high pressure turbopumps to indirectly survey temperature loads on the turbines. Further measures could be pressures of the preburner feed flows at appropriate locations of the thrustchamber and the rotational speed of the turbopumps. This is similar to the proposal in [41] for the SSME, where the standard sensors should be supplemented with additional temperature and pressure measurements for an advanced control scheme, with the aim of extending the life expectancy of engine components.

The HMS independently provides input for the engine emergency control and collection of huge operations data sets for maintenance prediction and support. The latter is to be stored with high sample rate in redundant form ‘on-engine’ for download after flight. Internal flow conditions, thermal and mechanical load data including vibrations can be used for automated post-flight assessment, implementing machine-learning algorithms. If such an approach is consequently followed already during development testing, a significant improvement in rocket engine reliability and robustness can be expected.

Current work focuses on the elaboration of the simulation environment modelling the transient behavior of the components involved in the cycle definition. Some components are modelled similar to those in [44]. For the turbopump components (pump and turbine section) the available SiW tabulated design data is used to obtain torque and power.

Specific effort was put into the modelling of the combustion devices (preburners and main combustion chamber). At this stage a simplified approach is used to obtain combustion data. Depending on the mixture ratio we have to distinguish between fuel-rich, oxidizer-rich and stoichiometric combustion. At this stage we do not yet consider additional combustion products beyond the formation of water and, depending on the mixture ratio, molecular O_2 or H_2 in the exhaust gas. Based on the exhaust gas composition, the mixture gas constant and the specific heat capacities are determined. The temperature dependency of these gas properties is considered by using polynomial functions as in [45].

For a transient simulation of the combustion process the derivative of the mass inside the combustion chamber is determined by the difference between inflow and outflow. An integration of this derivative yields the gas mass inside this volume and its density and pressure assuming permanently choked flow conditions at the throat section. This assumption is justified by the fact that no startup simulations shall be performed at this stage but only the transition from one operating point to another. A linear correlation between mixture ratio and combustion temperature is used for the gas generators which is sufficiently precise within the domain of operations of these combustion devices. For the main combustion chamber the correlation is quadratic.

While an almost exact reproduction of the steady mass flow rate was achieved (compare example of oxidizer-rich preburner Figure 14), a residual discrepancy remains for other parameters such as the chamber pressure.

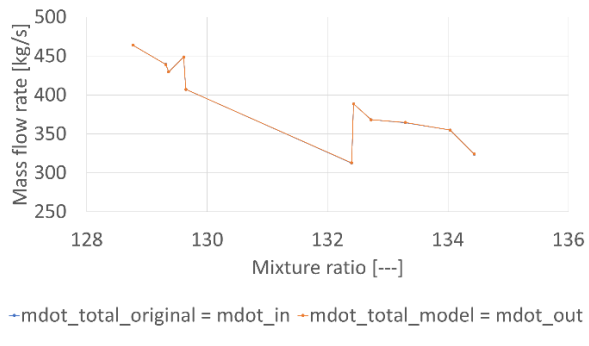

Figure 14: Total mass flow rate model vs. original data

The regenerative cooling system is modelled identically. Only a global heat flow rate from the hot gases through the wall into the cooling liquid (hydrogen) is determined. Fluid density at the outflow is modelled by the Peng-Robinson equation. Temperature dependency of the specific heat capacities is based on the polynomial model by [46].

The next step is to complete the component lists and then combining these to a full transient cycle simulation environment to be used for closed-loop control simulation.

2.5 SLME performance estimation

2.5.1 Cycle calculation models

A computer program used in the early phases of the SLME cycle analysis up to 2018 is lrp2, based on the modular program SEQ [30] of DLR. Since the 1990ies this powerful tool had been significantly upgraded. The modular aspect of the program allows for a quick rearrangement of the engine components, specifically the turbine and pumps assembly. After selection and sui-

table arrangement of the components in an input file, the program calculates the fluid properties sequentially according to the specific thermodynamic processes in the components, through which the fluid flows. Each constraint yields a nonlinear equation. This results in a system of nonlinear equations (or rather dependencies) which is solved by an external numerical subroutine.

The commercially available program RPA [31] Version 2.3.2 had been subsequently used for the preliminary analyses of the SLME and for further refinement of component definition. RPA is capable of predicting the delivered performance of a thrust chamber using semi--empirical relations [31] to obtain performance correction factors, including:

- performance loss due to finite-rate kinetics,
- divergence loss,
- performance loss due to finite-area combustor,
- performance change due to nozzle flow separation.

Those factors are relevant for the SLME design. The RPA engine cycle analysis module is capable of analyzing the operational characteristics of engine configurations, performing a power balance of the turbomachinery to achieve a required combustion chamber pressure [31]. The full-flow staged-combustion cycle (FFSC) which is the reference mode for the SLME is included in RPA, though, not the same as in Figure 1.

The lrp2 program is significantly more flexible in the arrangement of flow paths inside the engine than RPA 2.3.2. However, this complicates the user input and slows convergence of lrp2. During the SLME de-risking study, the lack of expander turbine modeling in RPA in combination with fixed flow paths turned out as a problem because the LPFTP boost pump could not be correctly modelled. This has an impact on the calculated conditions in the FR-preburner which requires a shift in mixture ratio to keep TET-targets. Some internal flow conditions were hence inaccurate, influencing the preliminary sizing of components. The implementation of AxSTREAM® corrected data in certain operating points. RPA offers more sophisticated performance estimation methods for nozzle expansion than the other mentioned cycle analysis tools.

The recent updates of SLME-analyses are based on calculations using a prototype version of lrp3, a newly developed steady-state rocket engine cycle analysis program. DLR's lrp3 should offer unrestricted architectural flexibility by propagating real fluid states across a modular network of components. The program can represent the full SLME flow diagram using discrete nodes – including pumps, turbines, valves, splitters, heat exchangers, gas generators/preburners and the main combustion chamber. By parsing the connections between the nodes, lrp3 performs a topological graph-based execution, utilizing Kahn's algorithm [33] to dynamically determine the correct component evaluation order. Critically, this modularity allows the user to combine a heat exchanger and a turbine to model an expander turbine for the SLME LPFTP.

The real fluid states are updated at each component using the CoolProp library [34], which accurately tracks enthalpy, entropy, temperature and density. Efficiency losses in the pumps and turbines are added as heat, increasing the fluid's enthalpy and temperature. Future integration of NIST REFPROP [35] is planned to expand this capability to propellants not featured in CoolProp, such as RP-1.

Also in lrp3, the gas generators and main thrustchamber combustion and one-dimensional nozzle expansion are currently calculated with RPA 2.3.2 connected via RPA's scripting utility. This approach allows including estimation of losses according to correction factors for the effects as listed above. In the future, this fast and straight-forward way might optionally be replaced by interfaces with more sophisticated tools like TDK or even CFD (see example calculations of the SLME thrustchamber in section 2.5.3).

To resolve the highly coupled, non-linear system of equations, lrp3 uses a normalized Jacobian solver. While its primary function is to strictly balance the mechanical power across the turbomachinery shafts, the solver's flexible architecture allows for the integration of custom constraints, such as specific preburner temperatures. The runtime until convergence for the SLME for each point in its operational domain (3 shaft balances, 2 preburner temperature targets to be fulfilled) is typically below 1 minute.

2.5.2 Operational domain and performance

The operational domain of the SLME remains the same as described in [9]. The different RLV-concepts using the SLME as its reference engine in the design studies summarized in [9 - 17] are all functioning at one or several of the nominal operations points O1, O2 and O3.

The calculated SLME operational domain is shown in Figure 15. The extreme points of the domain (E1 to E8) define the ultimate safe operation limits of the SLME with all its subcomponents. The MR-range extends from 5 to 7 and is realized mainly by adjusting the LOX-flow (up to ± 18%). Maximum LH2 massflow variation within the domain is less than ± 8%. This is a preliminary design decision which could be somehow adjusted based on future analyses. The SLME extends up to a maximum chamber pressure of 18 MPa. This value is in no way excessive compared to preceding LOX-LH2 engine developments as the SSME [36], RD-0120 [9] or Raptor 2 and 3 [1, 16].

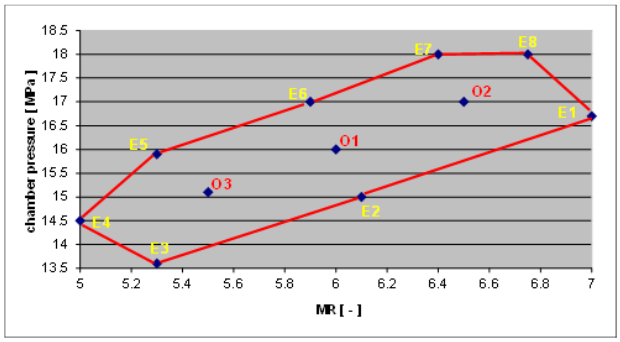

Figure 15: Calculated SLME operational domain

Figure 16 and Figure 17 show the respective FPRB and ORPB pressures against their own O_2 mass flows, as the latter are intended to be used for SLME engine control (Figure 1 and section 2.4.6). The fuel-rich turbine operates at a slightly higher, still moderate average pressure ratio compared to the oxygen-rich turbine (approximately 1.29 compared to 1.21). This drives the FRPB to higher overall operating pressures (range from

19 to 25.5 MPa) compared to the ORPB (range 18 to 24 MPa). The FRPB operates at mixture ratios between 0.65 and 0.675, while the ORPB varies between 135 and 142. These mixture ratios lead to O_2 mass flows between 36.5 and 43 kg/s in the FRPB and between 325 and 475 kg/s in the ORPB. Note, all these values are based on simplified one-dimensional combustion models assuming chemical equilibrium.

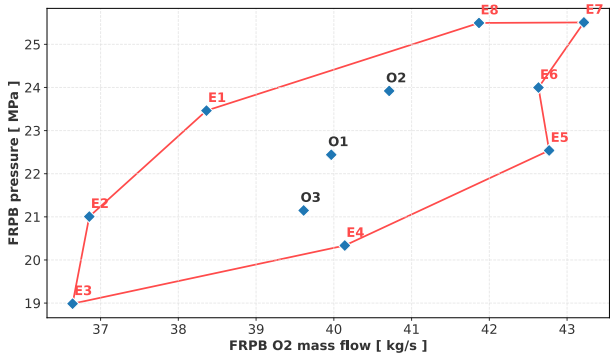

Figure 16: FRPB pressure over FRPB O_2 mass flow

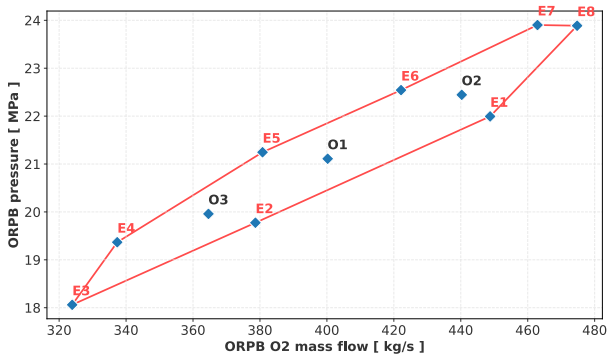

Figure 17: ORPB pressure over OPRB O_2 mass flow

2.5.3 Thrustchamber performance

Flow expansion in the nozzle is essential for an efficient SLME and, therefore, adequate, more refined simulations move into focus. Still on fast engineering level, the actual nozzle contour is considered in two-dimensional, rotational symmetric analyses for which the tools TDK and OpenFOAM are employed.

The classic NASA-funded TDK code is capable of two-dimensional equilibrium, frozen, or kinetic nozzle performance calculations with boundary layer effects [42]. The computational portion of TDK consists of six modules: one-dimensional equilibrium (ODE), one-dimensional kinetic (ODK), transonic flow (TRANS), method of characteristics (MOC), and two boundary layer modules (BLM and MABL). The BLM module calculates compressible laminar and turbulent wall boundary layers in axisymmetric nozzles. Both MABL and BLM use the Cebeci-Smith eddy viscosity model to model the turbulent boundary layer [43].

Additional simulations were performed using the open-source CFD tool OpenFOAM with the sonicFoam solver for transient, compressible flow. A three-dimensional, rotationally symmetric configuration was considered, where a 180° sector of the geometry was modeled. The computational grid comprised approximately 3.9×10^6 cells, predominantly hexahedral, with a minor fraction of prismatic and polyhedral elements. Laminar flow conditions were assumed.

At the nozzle inlet, fully homogeneous hot H_20 gas at total pressure of 15.49 MPa and total temperature of 3572.7 K were prescribed, derived from the RPA2.3.2 calculations at chemical equilibrium for O1. The specific heat ratio is set to $\gamma = 1.16$ without adaptation during expansion. The outlet was modeled using a wave-transmissive boundary condition with sea-level ambient pressure of 101325 Pa, while zero-gradient conditions were applied for velocity and temperature. Symmetry boundary conditions were imposed at the sector boundaries, and the nozzle walls were treated as slip boundaries.

The governing equations were solved in a transient manner using the finite volume method, and the simulation was advanced in time until a quasi-steady state was reached. A typical results plot of this inviscid calculation is visible in Figure 18.

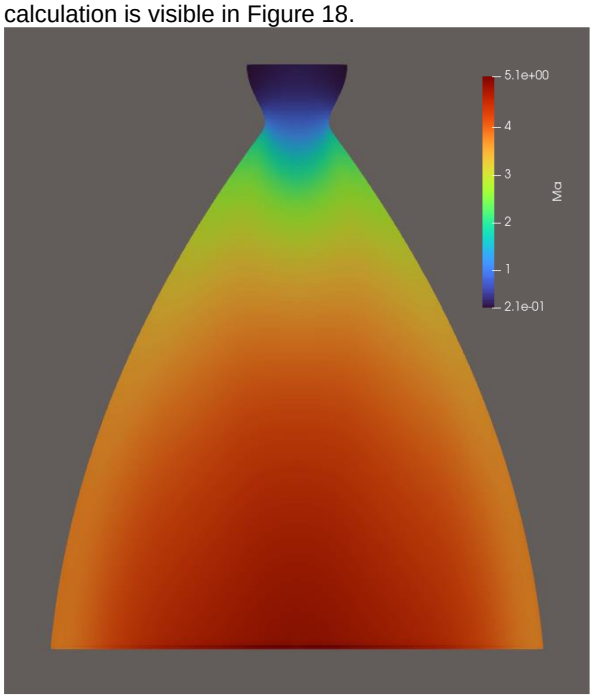

Figure 18: Mach-number distribution in SLME thrustchamber with ε=33 in inviscid OF simulation

In Figure 19 comparisons are plotted for the flow conditions in the exit plane obtained by the two different tools TDK and OpenFOAM. A relative radius of 0 represents the nozzle centerline while 1 is at the nozzle wall. Note the effect of the boundary layer in the TDK curves adjacent to the wall.

Results of the engineering tools are in acceptably good agreement under the consideration that the physical representation of the flow and gas properties is quite diverse for the methods. Both tools are intended to be used in future analyses and potentially in the refinement of the SLME nozzle contour. A fast engineering analysis, as available with TDK, enables a rapid variation of potential geometries in combination with several assumptions on regenerative and film cooling or wall roughness. CFD is intended to be used in subsequent steps for validation of such engineering data.

The wall temperature distribution from the preliminary thrustchamber sizing as presented in Figure 3 has been used as the wall boundary condition input for the TDK-calculation of O1. Figure 20 presents the velocity ratio through the boundary layer shortly behind the throat

section. The typical profile of a turbulent boundary layer is visible. Thickness of the BL at this point is roughly between 6 and 9 mm.

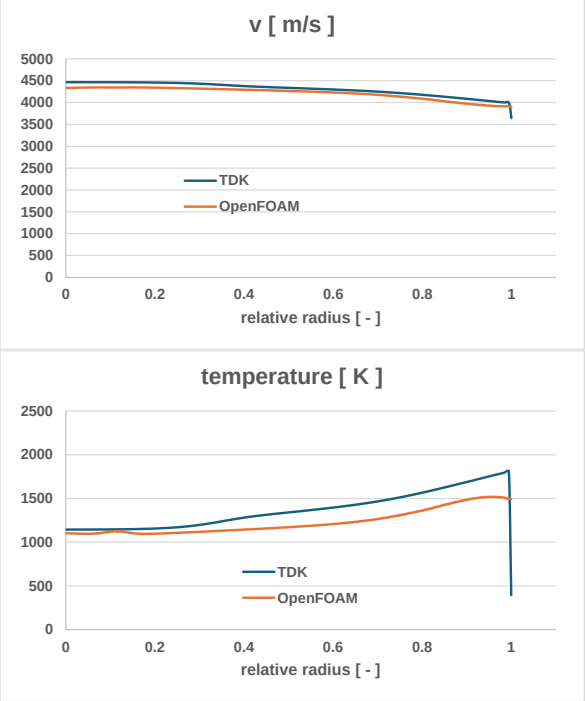

Figure 19: Comparison TDK with OF for flow conditions in nozzle exit plane over relative radius

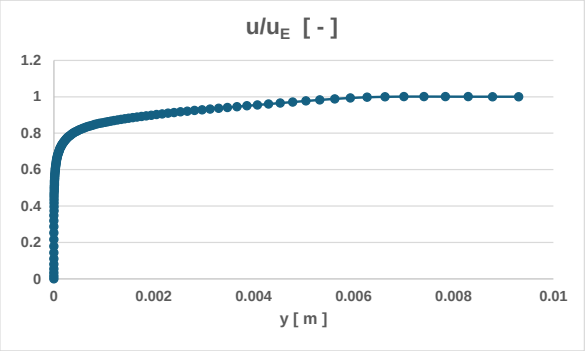

Figure 20: TDK calculated boundary layer velocity ratio at x= 5.28 cm behind throat

In a similar way Figure 21 shows the velocity ratio and Mach-number close to the nozzle exit. The thickness of the BL is now between 2 and 3 cm. The wall temperature close to the nozzle exit is kept at the predefined value of 580 K. This is an assumption based on previous simplified analyses. Actual values can be iterated by coupled, iterative analyses and will be part of future refined SLME thrustchamber design.

2.5.4 Engine performance

The AxSTREAM® analyses of all turbopumps conducted by SoftInWay and with major results presented in the previous section 2.4.4 and line pressure loss estimation have been used for engine models applied to RPA2.3.2 and new lrp3-cycle calculations. The efficiencies estimated by the preliminary AxSTREAM® design are influencing the assumptions in the cycle analyses. While the RPA-calculations assumed chemical equilibrium expansion in the complete nozzle, lrp3 applied frozen chemistry starting at low expansion ratio. The SLME flow scheme as shown in Figure 1 is the reference for all these cycle calculations.

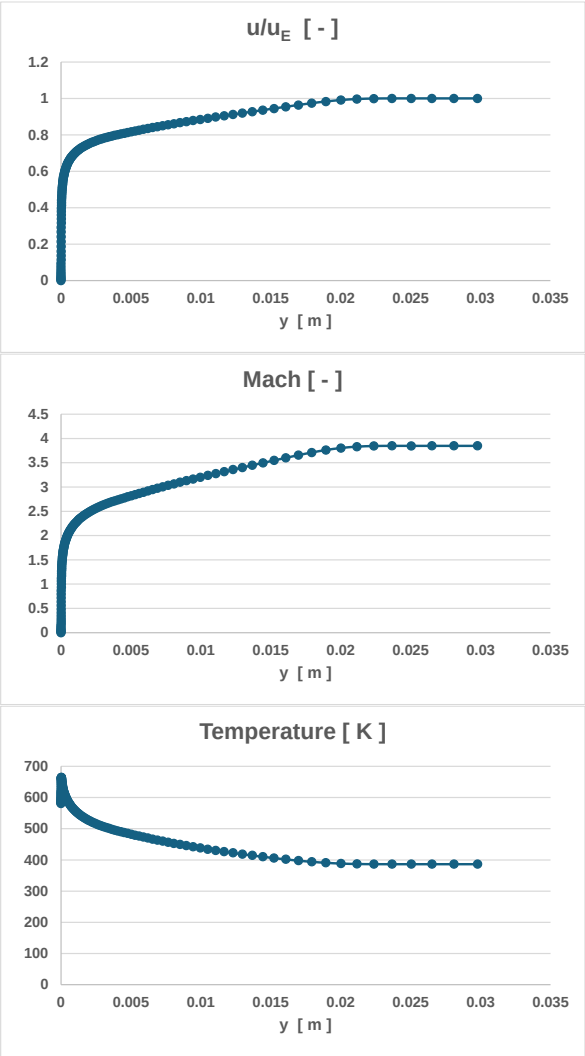

Figure 21: TDK calculated boundary layer conditions close to nozzle exit

Table 9 gives an overview about major SLME internal operation and engine performance data for the three nominal operating points as obtained by RPA cycle analyses. Performance data are presented for the two different nozzle expansion ratios of the SpaceLiner: 33 and 59.

Preburner combustion temperatures or TET in the full domain are kept in a relatively small range between 740 K to 780 K. The required preburner and hence turbopump discharge pressures are calculated by RPA using computed and estimated pressure drops in lines, valves and injectors. This impacts mainly the O_2 path because of the applied engine control logic and related valves placement. OTP-discharge pressure is raised by up to 3 MPa in comparison with [8]. Both preburners operate at similar pressure levels up to 25.9 MPa. However, the pumps are different: the OTP discharge reaches now up to 32.16 MPa at point O2 while HPFTP goes to 35.8 MPa because the complete hydrogen is directed first through the regenerative cooling before reaching the FRPB.

The lrp3 results in Table 10 converge close to RPA but with notably increased pressure levels on the fuel-rich side and slightly reduced levels on the ox-rich side.

Table 9: SpaceLiner Main Engine (SLME) technical data from RPA2.3 numerical cycle analysis

Operation point	**O1**	**O1**	**O2**	**O2**	**O3**	**O3**
Mixture ratio [-]	6		6.5		5.5	
Chamber pressure [MPa]	16		16.95		15.1	
Fuel-rich Preburner pressure [MPa]	23.9		25.7		22.6	
Oxidizer-rich Preburner pressure [MPa]	23.9		25.9		22.66	
Fuel-rich Preburner TET [K]	760		770		760	
Oxidizer-rich Preburner TET [K]	760		771.4		760	
HPFTP discharge pressure [MPa]	33.4		35.8		32.2	
OTP discharge pressure [MPa]	29.5		32.16		28.2	
Mass flow rate in MCC [kg/s]	513.5		555		477.65	
c* [m/s]	2310.28		2271.34		2343.45	
Expansion ratio [-]	**33**	**59**	**33**	**59**	**33**	**59**
c_F in vacuum [-]	1.8546	1.9057	1.8712	1.9255	1.8374	1.8855
c_F at sea level [-]	1.6381	1.5187	1.6671	1.561	1.6081	1.4755
Specific impulse in vacuum [s]	436.9	448.95	433.39	445.97	439	450.56
Specific impulse at sea level [s]	385.9	357.77	386.1	361.5	384.2	352.6
Thrust in vacuum per engine [kN]	2200	2260.68	2356	2427.28	2056.7	2110.49
Thrust at sea level per engine[kN]	1943	1801.55	2111	1967.32	1800	1651.56

Table 10: SpaceLiner Main Engine (SLME) with ε=33 technical data from lrp3 numerical cycle analysis

Operation point	**O1**	**O2**	**O3**
Mixture ratio [-]	6	6.5	5.5
Chamber pressure [MPa]	16	17	15.1
Fuel-rich Preburner pressure [MPa]	24.9	26.4	23.6
Oxidizer-rich Preburner pressure [MPa]	23.6	24.9	22.5
Fuel-rich Preburner TET [K]	760	770	750
Oxidizer-rich Preburner TET [K]	760	770	750
HPFTP discharge pressure [MPa]	34.4	35.9	33.1
OTP discharge pressure [MPa]	28.4	29.7	27.3
Mass flow rate in MCC [kg/s]	513.5	555	477.7
c* [m/s]	2315.8	2276.7	2349.5
c_F in vacuum [-]	1.8497	1.8618	1.8354
c_F at sea level [-]	1.6331	1.6577	1.6060
Specific impulse in vacuum [s]	436.8	432.2	439.7
Specific impulse at sea level [s]	385.6	384.8	384.8
Thrust in vacuum per engine [kN]	2199.8	2352.5	2060.0
Thrust at sea level per engine[kN]	1942.2	2094.6	1802.6

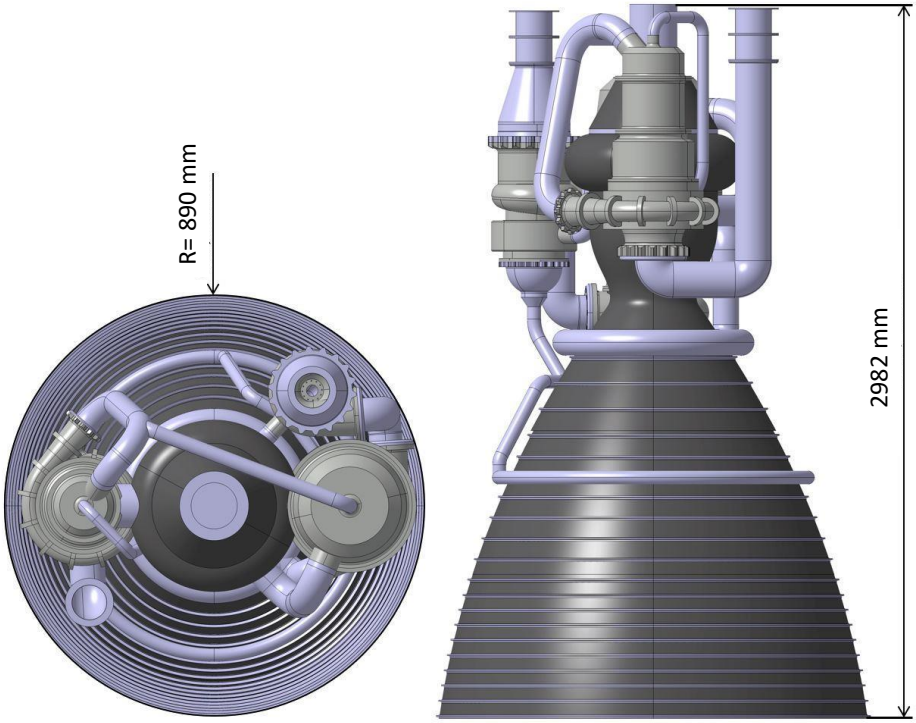

Figure 22: Overall size of SLME V7 with ε=33 as simplified CAD-model

The TDK performance summary with boundary layer ("second TDK/MABL SOLUTION") is listed in Table 11. Note the chamber pressure is iterated by TDK slightly above the input value of 160 bar.

Table 11: TDK calculated thrustchamber vacuum performance of SLME with ε=33 at O1

Mixture ratio [-]	6
Chamber pressure [MPa]	16.21
Mass flow rate in MCC [kg/s]	508.23
c* [m/s]	2352.4
c_F in vacuum [-]	1.8497
Specific impulse in vacuum [m/s]	4298.187
Specific impulse in vacuum [s]	438.29
Thrust in vacuum [kN]	2199.8

A comparison of the thrustchamber performance calculated by the three tools for O1 (Table 9, Table 10, Table 11) shows quite good agreement. It is to be acknowledged that some of the underlying methods and assumptions are the same or are very similar; all to be validated in future work. Vacuum Isp as calculated by TDK is up to 0.34% higher while vacuum thrust is lower by 0.7% than results of RPA2.3.2 or lrp3. The latter can be explained by the reduced mass flow of 508 kg/s (-1%) due to displacement effects of the BL. The reduced flow due to massflow displacement in the boundary layer had been disregarded in the early SLME thrustchamber contour definition and is not considered in the cycle tools RPA and lrp.

Future design maturations of the thrustchamber need to take into account the BL under different operational conditions including the film cooling with supercritical H_2 at the combustion chamber wall. Based on multiple engineering-level simulations, a refined thrustchamber geometry could be defined.

2.6 Engine Geometry and Mass

The size of the SLME in the smaller booster-type configuration (visible in Figure 22) has a maximum diameter of 1800 mm and overall length of 2982 mm. The larger upper stage SLME has a maximum diameter of 2370 mm and overall length of 3893 mm (Figure 23).

The de-risk study has not only refined the preliminary component sizing but also enabled an update of the engine mass assessment. The engine masses have been estimated at 3500 kg with the large nozzle and at 3218 kg for the booster stage nozzle with expansion ratio 33. This is an increase of roughly 4% compared to the previous versions [8]. These values are equivalent to vacuum T/W at MR=6.0 of 65.9 and 69.7. Some optimization potential exists, mainly with elimination of high-pressure LOX-lines by introducing an advanced annular ox-rich powerhead briefly discussed in the following section.

2.7 Outlook next generation architecture V9

In the early years of Space Shuttle operations, the MSFC sponsored several initiatives for improving this RLV. The focus was on the SSME, mostly on cost reductions and lifetime improvements. In [24] an FFSC derivative engine of the SSME is proposed with a very compact annular ox-rich preburner around the shaft connecting turbine and impeller/inducer [7, 24].

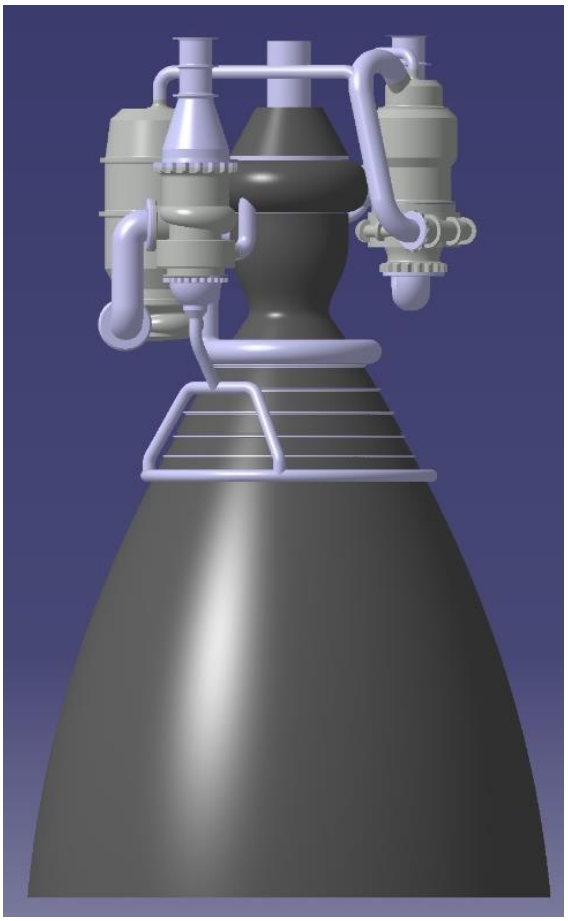

Figure 23: SLME V7 with ε=59 as simplified CAD-model

Such preburner design would allow for significant shortening of the powerhead assembly on the ox-rich side and eliminate some of the heavy high-pressure lines. The SpaceX Raptor makes use of such a lay-out with an assembly mounted right on top of the main combustion chamber. The turbine exhaust gas is directly fed to the injectors and hence into the combustion chamber. Alternative arrangements of the IPH-ox could be of interest as proposed in [25].

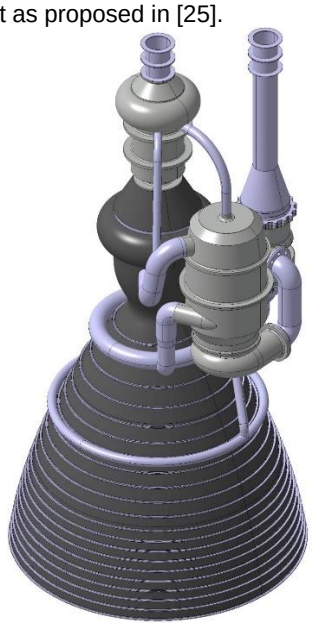

Figure 24: Preliminary CAD-model of SLME V9 with ε=33 and ox-rich power head on top of injector dome

This advanced powerhead assembly is potentially of major interest for the SLME and could significantly improve the weight penalty of FFSC mentioned in [27]. A preliminary lay-out of such a configuration, dubbed SLME V9, is presented in Figure 24. The overall length would increase by roughly 700 mm to almost 3.7 m. The turbopump and ducts arrangement as visible in Figure 24 is not finalized yet and likely will see some optimization in the future.

3 CONCLUSION

The full-flow staged combustion cycle around a moderate 16 MPa chamber pressure using LOX-LH_2 propellants had been selected early for the SpaceLiner Main Engine (SLME). After several years and many studies, this choice is maintained, the more as FFSC-architectures become increasingly popular. Beyond its original application, the SLME has been successfully implemented by DLR in several launcher system studies as RLV main propulsion. The engine can serve as a realistic baseline for the next generation of European staged-combustion cycle LOX-LH_2 rocket engines.

The engine operational domain is closely tracked by numerical analyses. The design with separate boost- and high-pressure pump on the LH_2 side and a single-shaft for inducer and impeller on the LOX side is maintained as the baseline and supported by preliminary turbopump sizing. The de-risk study for ESA has refined many engine component definitions with focus on the turbopumps and validated a mechanical architecture with pre-sizing of fluid lines.

The cycle and thrustchamber simulations have been extended to different numerical tools. All engine performance estimations converge in a small range. These tools are all remaining on the engineering design level but can significantly help in the refinement of the SLME design by running fast trade-studies.

The SLME masses in the 2200 kN thrust class are estimated at 3500 kg with large nozzle and at 3218 kg for typical booster stages. Advanced innovative engine architectures are under investigation which should improve the engine thrust-to-weight ratio while keeping high reliability for the entire 25 missions design life and low-cost manufacturing and maintenance.

The SLME is now one of the most sophisticated closed-cycle LOX-LH2 engine concepts in Europe and ready for further progress up to critical component validation.

4 ACKNOWLEDGEMENTS

The authors gratefully acknowledge the contributions of Ms. Carola Bauer, Ms. Carina Ludwig, Ms. Mona Carlsen, Mr. Jascha Wilken, Mr. Jan-René Haferkamp, Mr. Ryoma Yamashiro, Mr. David Gerson, Mr. Andreas Brückner, Mr. Francesco Cremaschi and Mr. Vincent Friesen to the preliminary design of the SLME and the SpaceLiner propulsion system.

5 REFERENCES

1. Herberhold, M.; Bussler, L; Sippel, M.; Wilken, J.: COMPARISON OF SPACEX'S STARSHIP WITH WINGED HEAVY-LIFT LAUNCHER OPTIONS FOR EUROPE, CEAS-Space Journal published online 28th May 2025, https://doi.org/10.1007/s12567-025-00625-8
2. Sippel, M.; Yamashiro, R.; Cremaschi, F.: Staged Combustion Cycle Rocket Engine Design Trade-Offs for Future Advanced Passenger Transport, ST28-5, SPACE PROPULSION 2012, Bordeaux, 7th – 10th May 2012
3. Yamashiro, R.; Sippel, M.: Preliminary Design Study of Staged Combustion Cycle Rocket Engine for SpaceLiner High-Speed Passenger Transportation Concept, IAC-12-C4.1.11, Naples, October 2012
4. Yamashiro, R.; Sippel, M.: Preliminary Design Study of Main Rocket Engine for SpaceLiner High-Speed Passenger Transportation Concept, ISTS2013-g-20, Nagoja, 2013
5. Yamashiro, R.; Sippel, M.: SpaceLiner Main Propulsion System, SART TN-010/2012, 2014
6. Sippel, M.; Schwanekamp, T.; Ortelt, M.: Staged Combustion Cycle Rocket Engine Subsystem Definition for Future Advanced Passenger Transport, Space Propulsion 2014, Cologne, Germany, May 2014
7. Sippel, M., Wilken J.: Preliminary Component Definition of Reusable Staged-Combustion Rocket Engine, Space Propulsion 2018, Seville, May 2018, Download Link
8. Sippel, M.; Stappert, S.; Pastrikakis, V.; Barannik, V.; Maksiuta, D.; Moroz, L.: Systematic Studies on Reusable Staged-Combustion Rocket Engine SLME for European Applications, Space Propulsion 2022, Estoril, Portugal, May 2022, Download Link
9. Sippel, M.; Dietlein, I.; Wilken, J.; Pastrikakis, V.; Barannik, V.; du Toit, T.H.J.; Moroz, L: System Aspects of European Reusable Staged-Combustion Rocket Engine SLME, Space Propulsion Conference, Glasgow, 20-23 May 2024, Download Link
10. Dietlein, I., Bussler, L., Stappert, S., Wilken, J., Sippel, M.: Overview of System Study on Recovery Methods for Reusable First Stages of Future European Launchers, CEAS Space Journal Volume 17, Issue 1, January 2025, https://doi.org/10.1007/s12567-024-00557-9
11. Wilken, J., Stappert, S.: Comparative Analysis of European Vertical-Landing Reusable First Stage Concepts, CEAS Space Journal Volume 17, Issue 1, January 2025, https://doi.org/10.1007/s12567-024-00549-9
12. Bussler, L., Dietlein, I., Sippel, M.: Comparative Analyses of European Horizontal-Landing Reusable First Stage Concepts, CEAS Space Journal Volume 17, Issue 1, January 2025, https://doi.org/10.1007/s12567-024-00572-w

13. Sippel, M. et. al.: A viable and sustainable European path into space – for cargo and astronauts, IAC-21-D2.4.4, 72nd International Astronautical Congress (IAC), Dubai, 25-29 October 2021, Download Link
14. Sippel, M.; Stappert, S.; Callsen, S.; Bergmann, K.; Dietlein, I.; Bussler, L.: Family of Launchers Approach vs. "Big-Size-Fits-All", IAC-22-D2.4.1, 73rd International Astronautical Congress, 18-22 September 2022, Paris, France, Download Link
15. Wilken, J., Herberhold, M.; Sippel, M.: COMPARATIVE ANALYSIS OF FULLY REUSABLE LAUNCH VEHICLES: FUEL CHOICES AND LANDING ARCHITECTURES, 11th European Conference for AeroSpace Sciences (EUCASS), Rome, 30th June to 4th July 2025
16. Sippel, M.; Wilken, J.; Dietlein, I.; Herberhold, M.; Bergmann, K., Bussler, L.: Evaluating launcher options for Europe in a world of Starship, Acta Astronautica 241 (2026) 455–472, https://doi.org/10.1016/j.actaastro.2026.01.018
17. Sippel, M.; Wilken, J.: Selection of propulsion characteristics for systematic assessment of future European RLV-options, CEAS Space Journal, Volume 17, Issue 1, January 2025, https://doi.org/10.1007/s12567-024-00564-w
18. Sippel, M., Stappert, S., Bayrak, Y.M.; Bussler, L.: Systematic Assessment of SpaceLiner Passenger Cabin Emergency Separation Using Multi-Body Simulations, CEAS Space Journal, Vol. 15, No. 6, November 2023, published online: 02 June 2023, https://doi.org/10.1007/s12567-023-00505-z
19. Espinosa-Ramos, A.; Taponier, V.: Towards a new class of engine for future heavy lift launch vehicles, Aerospace Europe Conference 2023 – 10TH EUCASS – 9TH CEAS, July 2023
20. Tan, Y-h et al.: Overview on Development of Liquid Rocket Engines for Heavy Launch Vehicles in China, IAC 2023-C4.1.1, 2023
21. Souchier, A. et al.: Snecma high thrust cryogenic engines for the next 20 years, AIAA 2004-3353, 40th AIAA/ASME/SAE/ASEE Joint Propulsion Conference and Exhibit, 2004
22. Jeaugey, I.; Montheillet, J.; Reichstadt, S.; Ghouali, A.; Dantu, G.: SYSTEM ENGINEERING PRESENTATION OF THE EUROPEAN STAGED COMBUSTION DEMONSTRATOR SCORE-D, SPACE PROPULSION 2012, Bordeaux, 7th – 10th May 2012
23. NN: RD-270, https://en.wikipedia.org/wiki/RD-270
24. Knuth, Wm. H.; Beveridge, J. H.: HIGH/VARIABLE MIXTURE RATIO OXYGEN/HYDROGEN ENGINES, N90-28637 in Summary of Booster Propulsion/Vehicle Impact Study Results (NAS8-36944), Boeing Aerospace, May 11, 1988
25. Knuth, W.; Crawford, R.; Litchford, R.: Integrated Modular Propulsion for Launch Vehicles, AIAA 93-1889, 29th Joint Propulsion Conference and Exhibit, Monterey, June 28-30, 1993
26. Meyer, L.; Nichols, J.; Jones, J.M.; Sabol, W.: Integrated Powerhead Demonstrator (booster hydrogen oxygen rocket engines), AIAA 96-4264, AIAA, Space Programs and Technologies Conference, Huntsville, AL, Sept. 24-26, 1996
27. S.D. PEERY - C.R. JOYNER - R.C. PARSLEY: Future Technology Directions and Payoffs for Reusable Cryogenic Propulsion, 5ème Symposium International, La Propulsion Dans Les Transports Spatiaux, Paris, 22-24 Mai 1996
28. NN: NEW ROCKET ENGINE COMBUSTION CYCLE TECHNOLOGY TESTING REACHES 100% POWER LEVEL, NASA press release, June 06, 2013, https://www.nasa.gov/news-release/new-rocket-engine-combustion-cycle-technology-testing-reaches-100-power-level/
29. Huzel, D. K., Huang, D. H.: Modern Engineering For Design Of Liquid-Propellant Rocket Engines, Washington, DC: American Institute of Aeronautics and Astronautics, (1992)
30. Goertz, C.: A Modular Method for the Analysis of Liquid Rocket Engine Cycles, AIAA 95-2966, 31st Joint Propulsion Conference 1995
31. Ponomarenko, A.: RPA – Tool for Rocket Propulsion Analysis, Space Propulsion 2014, Cologne, Germany, May 2014
32. Ponomarenko, A.: RPA: Tool for Rocket Propulsion Analysis, Thermal Analysis of Thrust Chambers, July 2012
33. Kahn, A.B., Topological sorting of large networks. Communications of the ACM, Volume 5, Issue 11, pages 558-562 (1962). https://doi.org/10.1145/368996.369025
34. Bell, I.H., Wronski, J., Quoilin, S., Lemort, V.: Pure and Pseudo-pure Fluid Thermophysical Property Evaluation and the Open-Source Thermophysical Property Library CoolProp. Industrial & Engineering Chemistry Research, Volume 53, Issue 6 (2014). https://doi.org/10.1021/ie4033999
35. Lemmon, E.W., Huber, M.L., McLinden, M.O.: NIST Standard Reference Database 23: Reference Fluid Thermodynamic and Transport Properties-REFPROP, Version 9.0. National Institute of Standards and Technology, Gaithersburg (2010) https://doi.org/10.18434/T4/1502528
36. NN: Space Shuttle Main Engine Orientation, Boeing Rocketdyne Propulsion & Power, Space Transportation System Training Data, June 1998
37. NN: Liquid Propellant Gas Generators, NASA Space Vehicle Design Criteria, NASA SP-8081, March 1972
38. NN: D4 – Preliminary design report for main components, 4000142002_23_NL_RK_D4, 2024
39. Sippel, M.; Dietlein, I.; Wilken, J.: SpaceLiner Subsystem Specification: SLME System Document, SL-SSS-SLME-SART-00040-1/1, SART TN-002/2024
40. Green, D.: What API Standards Govern Rotor Dynamics Analysis?, posted December 4, 2019, https://blog.softinway.com/what-api-standards-govern-rotor-dynamics-analysis/
41. Lorenzo, C. F., Musgrave, J. L.: Overview of Rocket Engine Control, NASA Technical Memorandum 105318, 9th Symposium on Space Nuclear Power Systems, New Mexico, USA, January 1992
42. Nickerson, G.R. et al: Two-Dimensional Kinetics (TDK) Nozzle Performance Computer Program, Vol. I, Engineering Methods, SN 130, Software and Engineering Associates, Inc., NASA Contract NAS8-39048, March 3I, 1993

43. Jankowsky, R.S.; Smith, T.D.; Pavli, A.J.: High-Area-Ratio Rocket Nozzle at High Combustion Chamber Pressure – Experimental and Analytical Validation, NASA/TP--1999-208522, June 1999
44. Pérez Roca, S.: Model-based robust transient control of reusable liquid-propellant rocket engines, HAL Id: tel-02888841, 2020
45. Manfletti, C.: Transient Behaviour Modelling of Liquid Rocket Engine Components, Shaker Verlag GmbH, ISBN 978-3-8322-8878-5, 2009
46. McBride, Bonnie J.; Zehe, Michael J.; Gordon, Sanford: NASA Glenn Coefficients for Calculating Thermodynamic Properties of Individual Species, NASA/TP--2002-211556, September 2002

Further updated information concerning the SART space transportation concepts is available at:
http://www.dlr.de/sart